Received: 19 September 2023 | *Revised:* 24 January 2024 | *Accepted:* 26 January 2024
DOI: 10.37917/ijeee.21.2.4 *Early View* | *December 2025*

Iraqi Journal for Electrical and Electronic Engineering
Original Article

Open Access
IJEEE University of Basrah College of Engineering

Optimal Hybrid Fuzzy PID for Pitch Angle Controller in Horizontal Axis Wind Turbines

Adnan Qahtan Adnan*, Mohammed Khalil Hussain
Department of Energy Engineering, University of Baghdad, Baghdad, Iraq

Correspondance
*Adnan Qahtan Adnan
Department of Energy Engineering, University of Baghdad, Baghdad, Iraq
Email: a.adnan1609@coeng.uobaghdad.edu.iq

Abstract
Wind turbine (WT) is now a major renewable energy resource used in the modern world. One of the most significant technologies that use the wind speed (WS) to generate electric power is the horizontal-axis wind turbine. In order to enhance the output power over the rated WS, the blade pitch angle (BPA) is controlled and adjusted in WT. This paper proposes and compares three different controllers of BPA for a 500-kw WT. A PID controller (PIDC), a fuzzy logic controller (FLC) based on Mamdani and Sugeno fuzzy inference systems (FIS), and a hybrid fuzzy-PID controller (HFPIDC) have been applied and compared. Furthermore, Genetic Algorithm (GA) and Particle swarm optimization (PSO) have been applied and compared in order to identify the optimal PID parameters (kp, ki, kd). The objective of GA and PSO is minimized the error signal in output power based on actual WS. The results for three different controllers show that the optimal hybrid FPIDC based on the Sugeno inference system with PSO produces the optimal results regard to reduce the error signal and stable output power under actual WS.

Keywords
Fuzzy Logic, PID, Hybrid Fuzzy-PID, Pitch Angle Control, Particle Swarm Optimization, Genetic Algorithm.

I. Introduction

Renewable sources of energy including solar, wind, geothermal, and bio fuels have become more popular due to environmental degradation and global warming [1]. WT can categorized as horizontal-axis wind turbine (HAWT) and a vertical-axis wind turbine (VAWT). HAWT extracts more power than VAWT [2]. The main component of WT that directly affects output power and efficiency is BPA. The blade design has several factors, such as blade length, blade shape, and pitch control. The performance of WT can be enhanced when improving BPA controller [3]. BPA of WT is used to regulate the power generation from WT as well as minimize the fatigue load exerted on the turbine-related components. BPA control is typically used when WS is higher than the rated WS to maintain the power generation of WT at the rated power [4].

Detailed BPA controllers of WT can be either based on traditional or artificial intelligence controllers. The traditional PIDC has been used to improve the BPA of WT [5]. PIDC based on either conventional or sophisticated calculation can control the BPA system and keep the power generation of WT near to the set point in both with and without disturbances [6]. When the WS exceeds the turbine's rated speed, a PID controller is designed to manage the BPA of WT [7, 8]. On the other hand, in the advanced design approaches, modeling, simulation, and computational optimization are necessary. Therefore, PSO and GA are the most widely used techniques for optimizing nonlinear and highly complicated problems [9]. An intelligent Genetic algorithm (IGA) approach can find the optimal tuning of PID parameters for the BPA controller better than GA [10]. PSO and GA are compared to find the optimal tuning of PID parameters and the results shows PID controller based PSO has better output power flow and the dynamic response than PID controller based GA [11]. Furthermore, ant colony optimization (ACO), PSO, and classical Ziegler–Nichols (Z-N) algorithms have been compared to find

the optimal parameters of PID controller for BPA of WT and the results show PID based on ACO optimization provide the lowest error in output power generation than the other algorithms [12]. On the other hand, FLC is the most often used for controlling nonlinear systems. When obtaining an accurate mathematical representation of the system is complicated, FLC is becoming more popular due to it is ability to use expert knowledge in the control design as well as it can improve the flexibility of nonlinear systems in the presence of fluctuations or uncertainty. The comparison between FLC based on Mamdani FIS and PIDC for BPA controller in HAWT are presented and showed that FLC is effective in decreasing fluctuations and normalizing the output power better than PID controller [13–17]. Also, the output power generation of WT is stabilized when using FLC base on Sugeno FIS [18]. The hybrid FPIDC is a combination of FLC with PIDC. Furthermore, the hybrid FPIDC can reduce the overshoot of output power generation under different wind speed [19]. The hybrid FPIDC performed better BPA controller of WT than PIDC and FLC [20–22]. The hybrid FPIDC has been used for BPA controller and results for 1.5 MW WT show that the hybrid FPIDC can improve the performance of WT better than PIDC and FLC [23]. Optimal hybrid FPIDC based on GA has been applied and achieving improvements in output power and structure stability of Floating offshore wind turbines [24]. Also, GA is used to find the optimal tuning of PID parameters in optimal hybrid FPIDC based on Mamdani FIS for providing better power generation than PID controller without optimization [25].

This paper compares three different controllers for BPA based on specific actual WS: PIDC, FLC, and hybrid FPIDC have been used and compared to find the best controller. A 500-kw wind turbine system is built using MATLAB® 2022 Simulink with taking into account the effect of BPA. The novelty of this paper is the comparison between two FIS (Mamdani and Sugeno) for FLC in WT. Furthermore, PSO and GA are compared to determine the optimal parameter values (kp, ki, and kd) used for PID and hybrid FPIDC. The results demonstrate that the optimal hybrid FPIDC based on Sugeno FIS and PSO can show the optimal results in stable output power and error signal.

II. Characteristics of WT

Turbine speed must be controlled during the operation depending on WS and output power. This control technology works to protect turbine systems and increase output power in both high and low WS situations. As shown in Fig. 1, the output power of WT has four operation zones based on variable WS and BPA. In (I.) zone when the cut-in speed is higher than WS, the output power is zero. (II.) zone has the maximum power point tracking because it is between cut-in speed and

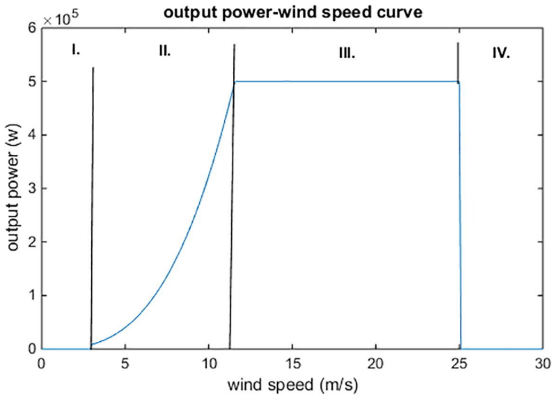

Fig. 1. Characteristic curve of WT [18].

rated speed. (III.) zone is between rated speed and cut-out speed. Finally, in (IV.) zone, WT is stopped because WS is beyond the cut-out speed [18]. The power coefficient (Cp) is a main factor in calculating the power generation of WT. In general, Cp depends on the tip speed ratio (λ) and pitch angle (β). As shown in Fig. 2, Cp describes how effectively WT generates power. (λ) and Cp are used to determine WT speed. Furthermore, (λ) and Cp changed based on different values of (β). Fig. 2 shows that when (β) is zero, Cp is maximum [18].

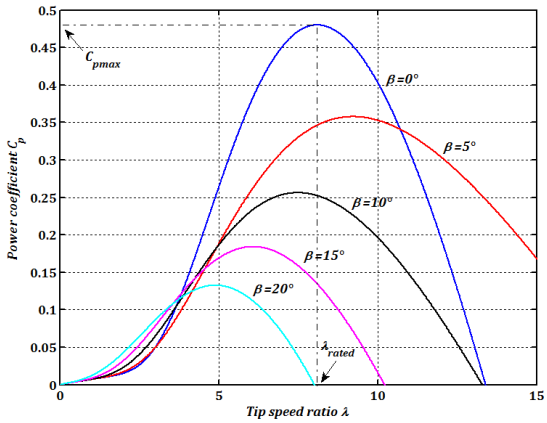

Fig. 2. Power coefficient in different BPA.

III. Mathematical Model of WT

This section explain the mathematical model of wind turbine including the effect of BPA. The following formula used to calculate the power generation of WT [18]:

$$P_w = 0.5\ \rho\ A\ v^3 \quad (1)$$

Where (P_w) is the wind power (Watt), (ρ) is the air density (kg /m^3), (A) is the blades swept area (m^2), and (v) is

WS (m/s). The mechanical power generation of WT can be calculated as below:

$$P_m = P_w C_p(\lambda, \beta) \tag{2}$$

The mechanical power (P_m) of WT is calculated by using Equations (1) and (2).

$$P_m = 0.5\,\rho\,A\,v^3\,C_p(\lambda, \beta) \tag{3}$$

Cp is nonlinear in most cases and it can change according to variations in WS as shown in the Equation below

$$C_p = 0.5\left(\frac{116}{\lambda_i} - 0.4\,\beta - 5\right)e^{\left(-\frac{21}{\lambda_i}\right)} + 0.0068\,\lambda \tag{4}$$

When (λ_i) value in (5) is swapped in (4), the Cp value is obtained. Here, the calculations are made simpler by using the value of the intermediate variable (λ_i), which is written as the following Equation:

$$1/\lambda i = 1/(\lambda + 0.08\,\beta) - 0.035/(3\,\beta + 1) \tag{5}$$

Tip speed ratio can be calculated based on the mechanical angular speed as follows:

$$\lambda = (w_{wt} * R) / (v) \tag{6}$$

where (R) is the radius of turbine blade (m) and (w_wt) is the rotor angular speed of the turbine (rad/s). Any modification in the rotor speed or WS in WT affects (λ) which varies Cp. These modifications also cause variations in the power output. The electrical power and mechanical torque in WT are shown below:

$$P_{el} = 0.5\,\rho\,A\,v^3\,C_p(\beta, \lambda)\eta_{gen} \tag{7}$$

$$T_m = P_el * w_{wt} \tag{8}$$

where (P_{el}) is the turbine electrical power (watt), (T_m) is the turbine mechanical torque (N.m), and (η_{gen}) is the generator efficiency.

IV. BPA Controllers

This section presents the controller of BPA in three different strategies: PIDC, FLC, and hybrid FPIDC. These controller strategies are used to maintain the power generation of WT in a stable region.

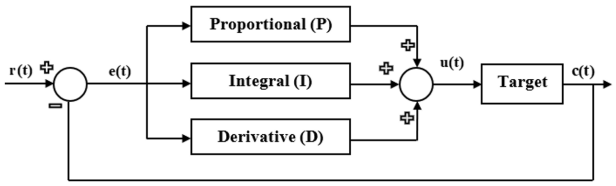

Fig. 3. Principal diagram of PIDC.

A. PIDC Design

The traditional PIDC is proportional (P), integral (I), and derivative (D). PIDC is used to create an output based on the controlled target [10]. Fig. 3 shows the principles of the traditional PIDC where u(t) is the out of control, c(t) is the output of controlling system, r(t) is the reference input, and e(t) is error. The output of the PIDC in the time domain is equivalent to the control input to the plant and is as follows:

$$u(t) = k_p e(t) + k_i \int e(t)dt + k_d \frac{de}{dt} \tag{9}$$

The control gains (k_p), (k_i), and (k_d) are constants and it must be determined during the design process.

B. FLC Design

This section explains the design and working principle of the FLC with two FIS (Mamdani and Sugeno). MATLAB Simulink is used to design the FLC includes, including fuzzification, defuzzification, inference system, and the rule base. In FLC, each object is given a membership degree in the range [0, 1] [26]. Error and error change are designated as two fuzzy input variables. The rule base and FIS specify the amount, of changes in angle based on the output variable. Mamdani and Sugeno FIS are used and compared. Fig. 4 shows the main parts of the FLC system.

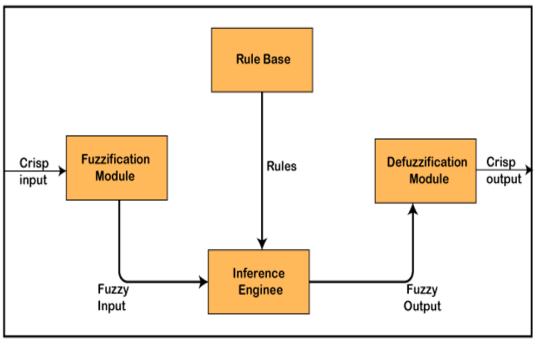

Fig. 4. The structure of FLC.

C. Hybrid FPIDC Design

For higher sensitivity and uncertainty , the hybrid fuzzy-PID control design have the input membership function as a Gaussian form, while the output membership function a triangular form. The hybrid controller based on FPIDC is illustrated in Fig. 5.

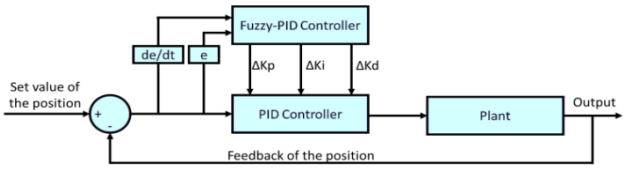

Fig. 5. The FPIDC design structure.

V. Optimization Techniques for optimal Controller

To obtain the optimal tuning for PID parameter values (k_p), (k_i), and (k_d) in this paper, PSO and GA are applied and compared to determine the optimal PID parameter of BPA controller. The five essential components in optimal tuning of PID parameters are defined as below:

1) Design Variables:

The main parameters of PID (kp, ki, kd) are defined as the design variables of the BPA controller in WT.

2) Objective Function:

Minimized (min) the error signal in the power generation and WS is the main objective function. The total error (E) is calculated based on the summation of the absolute errors obtained from power (P) and speed (W).

$$\text{minE}=\sum|(\,\mathrm{P_{ac}}-\mathrm{P_{ref}}\,)+(\,\mathrm{W_{ac}}-\mathrm{W_{ref}}\,)\,| \tag{10}$$

WhereP_{ac} and P_{ref} are actual and reference power outputs, while W_{ac} and W_{ref} are actual and reference WS.

3) Constraints:

The Constraints of the PIDC are defined based on the minimum and maximum levels of each parameter as given below:

$$\begin{pmatrix}\underline{\mathrm{K_{pmin}}}\le\mathrm{K_p}\le\overline{\mathrm{K_{Pmax}}}\\ \underline{\mathrm{K_{imin}}}\le\mathrm{K_i}\le\overline{\mathrm{K_{imax}}}\\ \underline{\mathrm{K_{dmin}}}\le\mathrm{K_d}\le\overline{\mathrm{K_{dmax}}}\end{pmatrix} \tag{11}$$

where K_p,$K_i$and K_d are the PID parameters; $\underline{K_{Pmin}}$ $\underline{K_{imin}}$, and $\underline{K_{dmin}}$ are the minimum levels of PID parameters and $\overline{K_{Pmax}}$,$\overline{K_{imax}}$ and $\overline{K_{dmax}}$ are the maximum levels of PID parameters.

4) Optimization Algorithms:

GA and PSO are used to determine the best PID controller parameters as the following.

A. Genetic Algorithm (GA)

The evolutionary algorithm based on a biological process used to optimize complex objective functions is called GA. GA uses seven steps to determine the best design variables: a parameter selection, decoding and encoding, population size, natural selection, combining, mating, and mutations. GA repeats the steps until the GA is converged [27].

B. Particle Swarm Optimization (PSO)

A population of interacting elements that can find the optimal design variables through the space of search is defined as PSO. Experience is defined as interacting elements (particles) traveling (flying) in quest of space to locate the optimum position. In the search space, each interacting piece saves the optimal location and neighborhood. PSO has seven steps to calculate the optimal design variables: defining the selection, finding the location, specifying the velocity vectors in each interacting element, finding the fitness values, calculating the locations, calculating the speed, and adjusting the location until the specified requirements are met [27, 28].

5) Optimization procedure

This section shows the procedure to calculate the optimal PID parameter of BPA controller in WT. First step is define the main component of the optimization algorithm : design variables, objective function, and constraints and apply optimization algorithm (GA or PSO) as explain in previous section. Second step is compute output power, pitch angle, and wind speed based on initial PID parameters for actual WS. third step is calculate the objective function (min(E)) based on Equation 10. Final step is finding the optimal value of (k_p, k_i, and k_d) after several iterations . Fig. 6 shows the flowchart of the optimization procedure to find the optimal PID parameter for the BPA controller of WT.

VI. Simulation Results and Discussion

Simulation model and results of 500-kw HAWT are presented in this section. WT system has been tested for three different controllers based on actual wind data as shown in Fig. 7.

A. Simulation Model of WT

In this paper, an advanced WT is created using MATLAB Simulink to provide the results of all operational variables and conditions for the input and output parameters. A simulink model for Cp has been created using Equations (4) and (5) to demonstrate how (λ) and (β) affect the amount of power produced by WT as shown in Fig. 8.

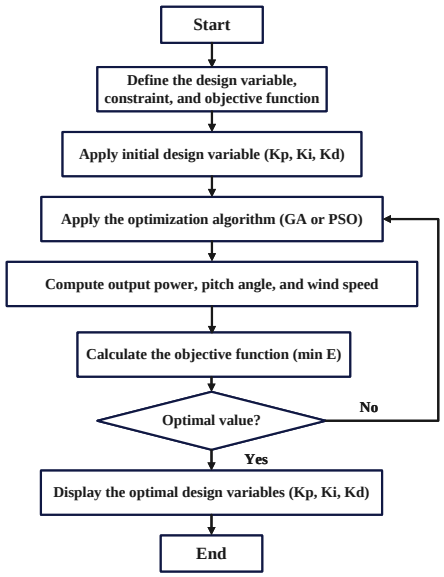

Fig. 6. Flowchart for the optimization process.

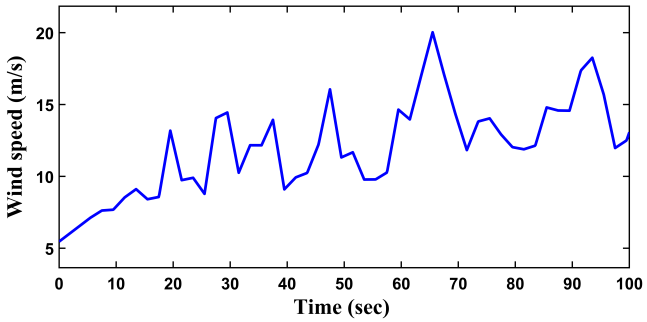

Fig. 7. WS for the 500 kW wind turbine.

According to Equations (3), (4), and (5), the variation in WT factors, such as WS, air density, swept area, and C_p affect the power production. Therefore, the Simulink model as shown in Fig. 9 is created by using Equations (7) and (8) and Fig. 10 shows the servo motor block based on the following formula (1/(s (s + 1))). Based on rated power circumstances, the generator efficiency is assumed to be 0.95 [29]. For relevant operations in MATLAB simulation, two MATLAB functions are defined in the Simulink model. The first one presents the cut-in WS while the second one presents the cut out WS. One of them is used to start the controller when working at the nominal WS, while the other function is used to stop the controller when working over the nominal WS.

Fig. 11 shows the complete model for WT system including three different controllers. Table I provides a list of the specifications used to create the 500-kW model [10]. The number of rotor blades on WT determines the ideal tip speed ratio (TSR).

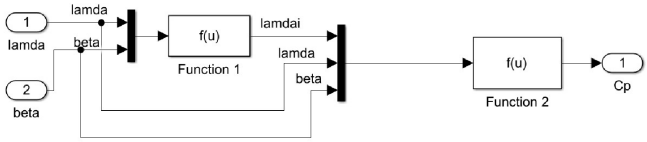

Fig. 8. Simulink model of power coefficient.

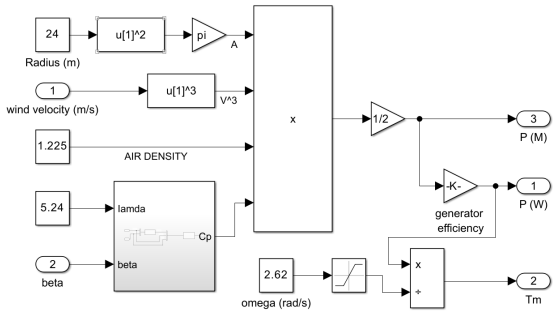

Fig. 9. Simulink model of WT system.

Fig. 10. Simulink model of servo motor.

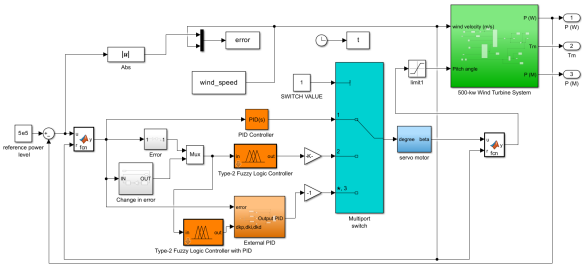

Fig. 11. Simulink model of WT system with all controllers.

In this paper, TSR is considered (4.19). If the airfoil is carefully built, the optimal TSR could be approximately 25% to 30% higher than this ideal value. The ideal TSR may exceed the stated limits depending on the type of profile utilized [30].

TABLE I.
SIMULATED WT SYSTEM PARAMETERS [10]

rated output power	500 kilo Watt
cut in WS	3 m/s
rated WS	12 m/s
cut out WS	25 m/s
diameter of the rotor	48 m
turbine blade number	3
rated rotor speed	30 rpm
range of rotor speeds	10–30 rpm
gearbox rate	01:50
generator type and number	PMSG - 2

B. Controller Model of WT

In this paper, three different controllers have been applied and compared to find the best controller of BPA: PIDC, FLC, and hybrid FPIDC.

1) Optimal PIDC

Figs. 12, 13, and 14 show the output power, pitch angle, and power error when PIDC is used. These results demonstrate that PSO-based optimal PID provides better results than GA in terms of output power and error between the reference and actual WS.

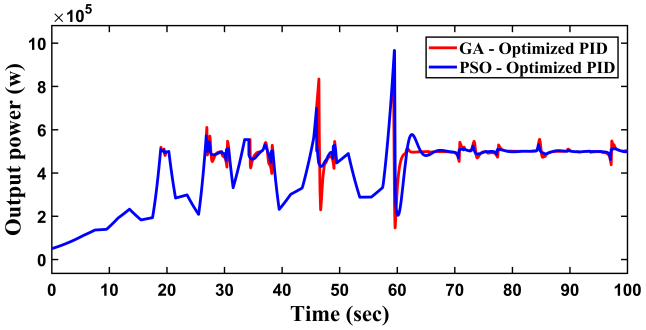

Fig. 12. Output power in PID-GA and PID-PSO.

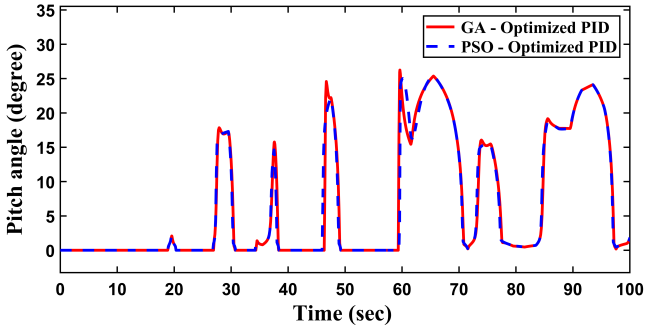

Fig. 13. Optimal BPA in PID-GA and PID-PSO.

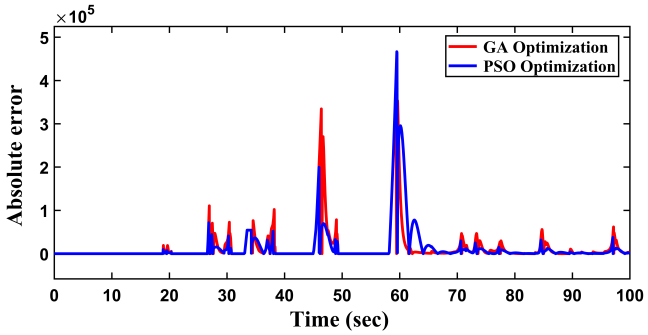

Fig. 14. Absolute Error in PID-GA and PID-PSO.

2) Fuzzy Logic Controller

FLC is used based on two FIS: Mamdani and Sugeno. Fig. 15 shows the input of FLC (error and derivative of error) as membership functions. Fig. 16 displays the amount of change in pitch angle for only Mamdani system. Table II provides a list of properties for Mamdani and Sugeno, these properties are used in the design of FLC. The Mamdani and Sugeno FIS are similar, however, the main difference is Sugeno FIS does not involve clipping in output membership function because the Sugeno FIS output are either linear or constant.

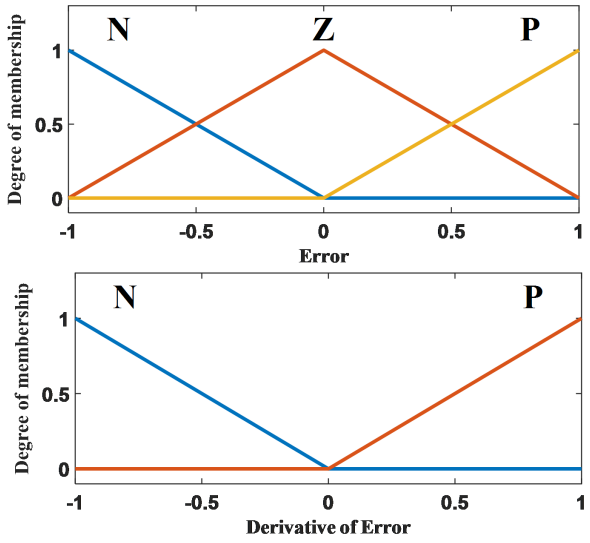

Fig. 15. The input variables fuzzy sets.

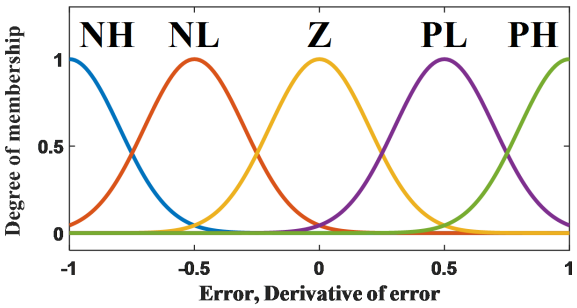

Fig. 16. The change in output variable fuzzy sets.

TABLE II.
PROPERTIES OF MAMDANI AND SUGENO FIS

Properties	Mamdani	Sugeno
And Method	Min	Min
Or Method	Max	Max
Implication Method	Min	Prod
Aggregation Method	Max	Sum
Defuzzification Method	Centroid	Weaver

As shown in Fig. 17, the fuzzy controller surface for Mamdani and Sugeno FIS illustrates the relationship between input and output variables as three-dimensional graphics. The rule base for the two FIS is the same as shown in Table III.

TABLE III.
FLC RULES FOR MAMDANI AND SUGENO

Pitch angle change		Derivative of error	
		Negative	Positive
Error	Negative	PB	PS
	Zero	Z	Z
	Positive	NS	NB

Two input values have three linguistic levels for error and two linguistic levels for the derivative of error with the following names: negative (N), zero (Z), and positive (P). While five linguistic levels in the output value with the following names: positive big (PB), positive small (PS), zero (Z), negative small (NS), and negative big (NB). The comparison in output power for two FIS (Mamdani and Sugeno) is shown in Fig. 18 and the absolute Error is shown in Fig. 19. As shown in both of the Figs, Sugeno FIS has better stability and lower error signal than Mamdani FIS.

3) Optimal Hybrid FPIDC

Fig. 20 shows the fuzzification of FLC for Mamdani and Sugeno FIS. Fig. 21 shows the defuzzification of the output variables for Mamdani FIS. The input membership values have five linguistic levels with the following names: negative high (NH), negative low (NL), zero (Z), positive low (PL), and positive high (PH).There are five output linguistic levels: negative small (NS), negative medium (NM), negative medium-big (NMB), negative big (NB), and negative very-big (NVB). Sugeno output membership functions (MFs) are to be constant. The control rule for each parameter of PIDC has 25 specific rules, as shown in Table IVIV. The complete control rules of the hybrid FPIDC have 75 rules.

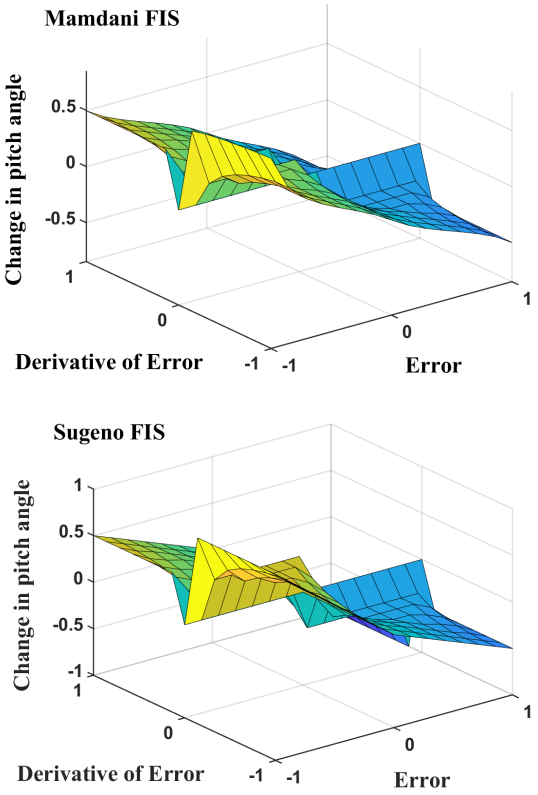

Fig. 17. FIS surface for Mamdani and Sugeno.

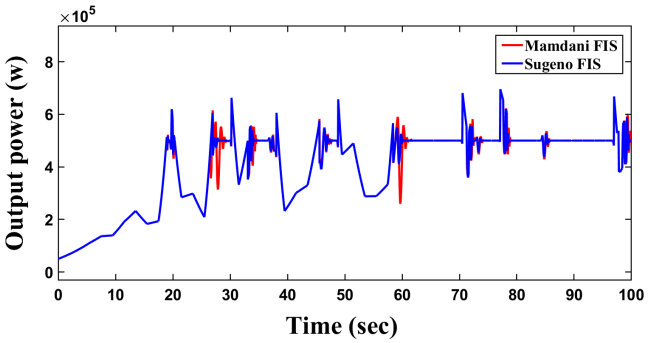

Fig. 18. Output power for Mamdani and Sugeno FIS.

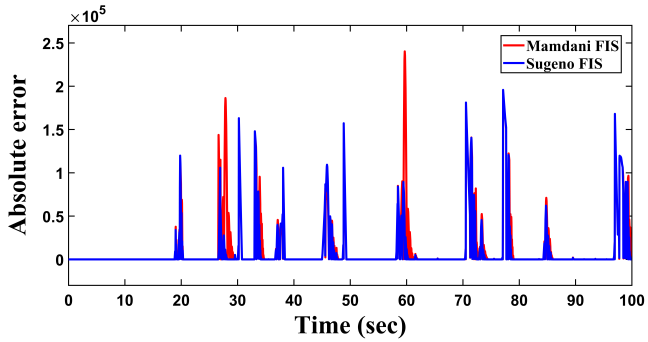

Fig. 19. Absolute Error for Mamdani and Sugeno FIS.

TABLE IV.
RULES FOR MAMDANI AND SUGENO FIS

Dkp		Derivative of error				
		NH	NL	Z	PL	PH
Error	NH	NS	NS	NS	NMB	NMB
	NL	NS	NM	NM	NB	NMB
	Z	NS	NM	NMB	NB	NB
	PL	NM	NM	NB	NB	NB
	PH	NMB	NMB	NB	NVB	NVB
Dki		**Derivative of error**				
		NH	NL	Z	PL	PH
Error	NH	NVB	NVB	NB	NB	NMB
	NL	NVB	NB	NB	NMB	NM
	Z	NVB	NMB	NMB	NB	NS
	PL	NM	NMB	NS	NB	NS
	PH	NS	NMB	NS	NVB	NS
Dkd		**Derivative of error**				
		NH	NL	Z	PL	PH
Error	NH	NS	NS	NM	NM	NMB
	NL	NS	NM	NM	NMB	NMB
	Z	NS	NM	NMB	NB	NVB
	PL	NM	NMB	NB	NB	NVB
	PH	NMB	NVB	NB	NVB	NVB

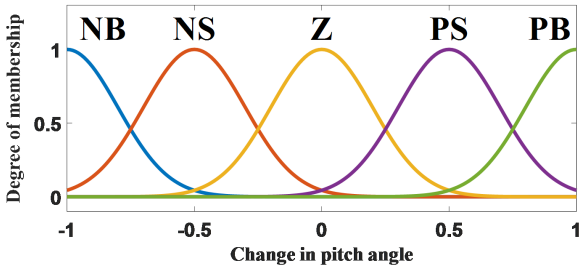

Fig. 20. The input variables fuzzy sets for hybrid FPIDC.

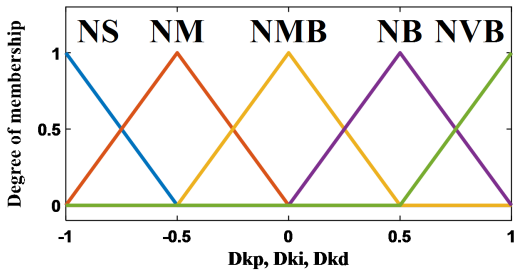

Fig. 21. The output variable fuzzy sets for hybrid FPIDC.

Since the Sugeno has better stability than Mamdani, Sugeno FIS has been only used in the hybrid FPIDC. Fig. 22 shows the output power for hybrid FPIDC using PSO and GA and Fig. 23 shows the optimal BPA. Furthermore, the Absolute error is shown in Fig. 24. Table V. compares the maximum and summation error for all controllers. According to this table, hybrid FPIDC has more consistent output power with lower error than other controllers. Also, Sugeno FIS and PSO for PID parameters provide the lowest error. The proposed controller can increase the life cycle and efficiency of WT. No BPA control is indicated when the WS is less than the rated value. As a result, controller performance can be obtained when transitioning from lower to higher rated speeds as well as from higher to lower rated speeds. As a result, the absolute error in each transition is high.

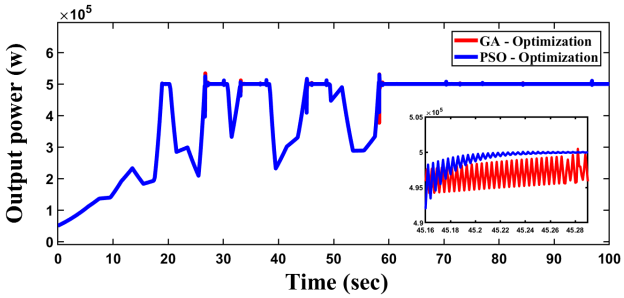

Fig. 22. Output power for hybrid FPIDC with GA and PSO.

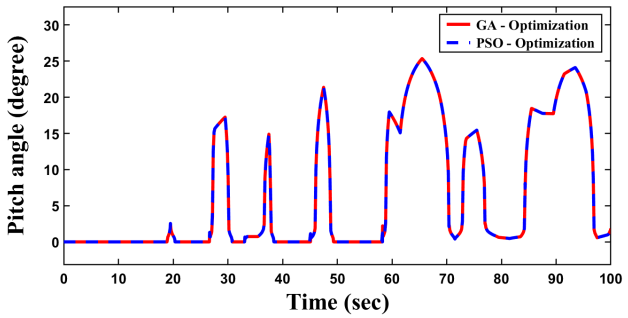

Fig. 23. Optimal BPA for hybrid FPIDC-GA and PID-PSO.

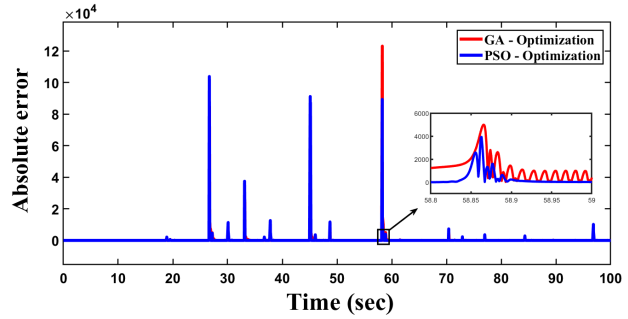

Fig. 24. Absolute error for hybrid FPIDC for GA and PSO.

TABLE V.
MAXIMUM ERROR AND SUMMATION ERROR

PIDC	Wind turbine power error	
	Summation error	**Maximum error**
GA	$1.4212 * 10^9$	$4.1095 * 10^5$
PSO	$1.3812 * 10^9$	$4.6654 * 10^5$
FLC	**Wind turbine power error**	
	Summation error	Maximum error
Mamdani	$1.3149 * 10^9$	$2.4022 * 10^5$
Sugeno	$9.9953 * 10^8$	$1.9576 * 10^5$
Sugeno HFPIDC	**Wind turbine power error**	
	Summation error	Maximum error
GA	$1.1749 * 10^7$	$1.2315 * 10^5$
PSO	$7.0370 * 10^6$	$1.0390 * 10^5$

VII. CONCLUSIONS

An optimal hybrid FPIDC based on the PSO algorithm was proposed in this paper for controlling BPA of WT system. The proposed controller is compared with an optimal PIDC and FLC. Two FIS (Mamdani and Sugeno) was used and compared to find the best FIS used in FLC. PIDC parameters (kp, ki, and kd) were optimized by using two different optimization methods (GA and PSO). The results demonstrate that the system is more stable when using the optimal hybrid FPIDC based on the Sugeno FIS and optimal PIDC parameters by using PSO. Finally, the optimal hybrid FPIDC system can produce a stable output voltage and increase the life cycle of WT.

CONFLICT OF INTEREST

The authors have declared no conflict of interest.

REFERENCES

[1] I. Daut, A. Razliana, Y. Irwan, and Z. Farhana, "A study on the wind as renewable energy in perlis, northern malaysia," *Energy Procedia*, vol. 18, pp. 1428–1433, 2012.

[2] J. Fadil, M. Ashari, *et al.*, "Performance comparison of vertical axis and horizontal axis wind turbines to get optimum power output," in *2017 15th international conference on quality in research (QiR): International Symposium on Electrical and Computer Engineering*, pp. 429–433, IEEE, 2017.

[3] Y. El-Okda, M. S. Emeara, N. Abdelkarim, K. Adref, and H. Al Hajjar, "Performance of a small horizontal axis wind turbine with blade pitching," in *2020 Advances in Science and Engineering Technology International Conferences (ASET)*, pp. 1–5, IEEE, 2020.

[4] R. Hara, "Prediction of wind power generation output and network operation," in *Integration of Distributed Energy Resources in Power Systems*, pp. 109–131, Elsevier, 2016.

[5] X. Yao, X. Su, and L. Tian, "Pitch angle control of variable pitch wind turbines based on neural network pid," in *2009 4th IEEE conference on industrial electronics and applications*, pp. 3235–3239, IEEE, 2009.

[6] D. Zhang, P. Cross, X. Ma, and W. Li, "Improved control of individual blade pitch for wind turbines," *Sensors and Actuators A: Physical*, vol. 198, pp. 8–14, 2013.

[7] Z. J. Mohammed, S. E. Mohammed, and M. O. Mustafa, "Improving the performance of pitch angle control of variable speed wind energy conversion systems using fractional pi controller," in *2022 Iraqi International Conference on Communication and Information Technologies (IICCIT)*, pp. 209–215, IEEE, 2022.

[8] M. K. Dhar, M. Thasfiquzzaman, R. K. Dhar, M. T. Ahmed, and A. Al Mohsin, "Study on pitch angle control of a variable speed wind turbine using different control strategies," in *2017 IEEE International Conference on Power, Control, Signals and Instrumentation Engineering (ICPCSI)*, pp. 285–290, IEEE, 2017.

[9] X.-S. Yang, S. Koziel, and L. Leifsson, "Computational optimization, modelling and simulation: Recent trends and challenges," *Procedia Computer Science*, vol. 18, pp. 855–860, 2013.

[10] Z. Civelek, E. Çam, M. Lüy, and H. Mamur, "Proportional–integral–derivative parameter optimisation of blade pitch controller in wind turbines by a new intelligent genetic algorithm," *IET Renewable Power Generation*, vol. 10, no. 8, pp. 1220–1228, 2016.

[11] A. Khurshid, M. A. Mughal, A. Othman, T. Al-Hadhrami, H. Kumar, I. Khurshid, Arshad, and J. Ahmad, "Optimal pitch angle controller for dfig-based wind turbine system using computational optimization techniques," *Electronics*, vol. 11, no. 8, p. 1290, 2022.

[12] M. R. Sarkar, S. Julai, C. W. Tong, M. Uddin, M. Romlie, and G. Shafiullah, "Hybrid pitch angle controller approaches for stable wind turbine power under variable wind speed," *Energies*, vol. 13, no. 14, p. 3622, 2020.

[13] A. Macedo and W. Mota, "Wind turbine pitch angle control using fuzzy logic," in *2012 Sixth IEEE/PES Transmission and Distribution: Latin America Conference and Exposition (T&D-LA)*, pp. 1–6, IEEE, 2012.

[14] H. Kumar, A. Gupta, R. K. Pachauri, and Y. K. Chauhan, "Pi/fl based blade pitch angle control for wind turbine used in wind energy conversion system," in *2015 International Conference on Recent Developments in Control, Automation and Power Engineering (RDCAPE)*, pp. 15–20, IEEE, 2015.

[15] Z. Civelek, E. Çam, M. Lüy, and G. Görel, "A new fuzzy controller for adjusting of pitch angle of wind turbine," *The Online Journal of Science and Technology*, vol. 6, no. 3, p. 1, 2016.

[16] A. Abir, D. Mehdi, and S. Lassaad, "Pitch angle control of the variable speed wind turbine," in *2016 17th International Conference on Sciences and Techniques of Automatic Control and Computer Engineering (STA)*, pp. 582–587, IEEE, 2016.

[17] G. A. Aziz, "Simulation model of wind turbine power control system with fuzzy regulation by mamdani and larsen algorithms," *Al-Khwarizmi Engineering Journal*, vol. 13, no. 1, pp. 51–61, 2017.

[18] Z. Civelek, "Optimization of fuzzy logic (takagi-sugeno) blade pitch angle controller in wind turbines by genetic algorithm," *Engineering Science and Technology, an International Journal*, vol. 23, no. 1, pp. 1–9, 2020.

[19] Y. Qi and Q. Meng, "The application of fuzzy pid control in pitch wind turbine," *Energy Procedia*, vol. 16, pp. 1635–1641, 2012.

[20] Z. Civelek, M. Lüy, E. Çam, and N. Barışçı, "Control of pitch angle of wind turbine by fuzzy pid controller," *Intelligent Automation & Soft Computing*, vol. 22, no. 3, pp. 463–471, 2016.

[21] D. C. Vega, J. A. Marin, and R. T. Sanchez, "Pitch angle controllers design for a horizontal axis wind turbine," in *2015 IEEE International Autumn Meeting on Power, Electronics and Computing (ROPEC)*, pp. 1–6, IEEE, 2015.

[22] D. Pathak and P. Gaur, "A fractional order fuzzy-proportional-integral-derivative based pitch angle controller for a direct-drive wind energy system," *Computers & Electrical Engineering*, vol. 78, pp. 420–436, 2019.

[23] T. G. G/Meskel, T. T. Yetayew, and E. A. Workeye, "Pitch angle control for optimal power of horizontal axis variable speed wind turbines using fuzzy tuned pid controller," in *Advances of Science and Technology: 9th EAI International Conference, ICAST 2021, Hybrid Event, Bahir Dar, Ethiopia, August 27–29, 2021, Proceedings, Part I*, pp. 237–255, Springer, 2022.

[24] C. Serrano, J.-E. Sierra-Garcia, and M. Santos, "Hybrid optimized fuzzy pitch controller of a floating wind turbine with fatigue analysis," *Journal of Marine Science and Engineering*, vol. 10, no. 11, p. 1769, 2022.

[25] A. S. Pehlivan, B. Bahceci, and K. Erbatur, "Genetically optimized pitch angle controller of a wind turbine with fuzzy logic design approach," *Energies*, vol. 15, no. 18, p. 6705, 2022.

[26] L. A. Zadeh, "The concept of a linguistic variable and its application to approximate reasoning—i," *Information sciences*, vol. 8, no. 3, pp. 199–249, 1975.

[27] M. K. Hussain and B. M. Alshadeedi, "Optimal design of high voltage composite insulators with grading rings in different configurations," *Electric Power Systems Research*, vol. 221, p. 109493, 2023.

[28] A. M. Rasham, M. K. Hussain, and M. Majeed, "Optimal characteristics of wind turbine to maximize capacity factor," in *AIP Conference Proceedings*, vol. 2651, AIP Publishing, 2023.

[29] T. Corke and R. Nelson, *Wind energy design*. CRC Press, 2018.

[30] M. Yurdusev, R. Ata, and N. Çetin, "Assessment of optimum tip speed ratio in wind turbines using artificial neural networks," *Energy*, vol. 31, no. 12, pp. 2153–2161, 2006.